Chinese Chemical Letters 34 (2023) 107560

Contents lists available at ScienceDirect

Chinese Chemical Letters

journal homepage: www.elsevier.com/locate/cclet

Pyrolysis of single carbon sources in SBA-15: A recyclable solid phase synthesis to obtain uniform carbon dots with tunable luminescence

Xiaoqing Niu, Weijie Zheng, Tianbing Song, Zunhui Huang, Chunlei Yang, Liming Zhang, Wei Li, Huanming Xiong*

Department of Chemistry and Shanghai Key Laboratory of Molecular Catalysis and Innovative Materials, Fudan University, Shanghai 200438, China

ARTICLE INFO

Article history:
Received 29 January 2022
Revised 20 May 2022
Accepted 23 May 2022
Available online 27 May 2022

Keywords:
Carbon dots
Solid phase synthesis
SBA-15
Luminescence
Uniformity

ABSTRACT

Most of carbon dots (CDs) are synthesized in solutions, but the extensive use of solvents produces too much waste, needs complex purification and results in low yield. Particularly for the popular hydrothermal/solvothermal syntheses, safety issues hinder the large-scale production of CDs. Solid phase synthesis in air seems perfect to solve the above problems once for all, but nanoparticle growth in solid phase is always difficult to control. Here we suggest a new method to synthesize CDs in SBA-15 template, just by heating single carbon sources in air. Employing single carbon sources is important, which ensures both homogeneity of the nucleation and uniformity of the nanoparticle growth. The pores confinement of SBA-15 guarantees the uniform sizes of CDs, while the catalytic effect of SBA-15 accelerates the carbonization process of precursors. The products are easily extracted from the template by ethanol, and then the template can be recycled for the next synthesis after calcination. Various CDs are synthesized in this way by using different carbon sources and SBA-15 templates with different pore diameters, respectively. The results show that, the fluorescence properties of these CDs are determined by their composition and surface states, but not the particle sizes. This work opens a new avenue to synthesize uniform CDs in solid phase with high yield, low cost and tunable luminescence.

Carbon dots (CDs) have attracted broad interest in optoelectronics [1–3], biomedicine and sensors [4–8] due to their fascinating properties in the past two decades [9]. To date, various methods have been applied to prepare CDs [10], such as acidic exfoliation [11], electrochemical oxidation [12,13], plasma fabrication [14], solvothermal or hydrothermal method [15–17], microwave treatment [18,19], pyrolysis [20] and magnetic hyperthermia [21]. Most of the preparation are carried out in solvents, and some of them require high temperature/pressure and even special equipment, which limit the large-scale production of CDs with convenient operation and low cost [22]. Previous reports have disclosed that solvents always involve in the formation of CDs, leading to complicated by-products and inhomogeneous composition in CDs [23,24]. As a result, CDs synthesized from solutions usually need multistep purification, including dialysis and chromatographic separation. Besides, it is a big trouble to dispose of the solvents after reaction and purification, which is harmful to both health and environment.

Solid phase synthesis of CDs is expected to overcome all of the shortcomings caused by solvents, but in fact it is always difficult to control nanoparticle growth in solid phase. Some pioneer work reported CDs grow unevenly, agglomerate and even lose fluorescence without the dispersion and the protection of solvents [25,26]. To overcome these drawbacks, Liu *et al.* employed silica spheres as carriers to produce CDs in Ar atmosphere at 900 °C [27]. Gu *et al.* used metal-organic framework (MOF) as the template and glucose as the carbon source to prepare CDs by calcination [28]. Ortega-Liebana *et al.* synthesized CDs with uniform size through pyrolysis in a fluidized bed reactor in a short time [29]. These efforts realized the monodispersion of CDs [30–33], but luminescence properties of the products are poor, including low quantum yield, very broad emission band, excitation-dependent emission wavelength and main fluorescence in blue region. Moreover, these CDs usually cannot be separated without destroying the templates, and some of them lost fluorescence after separation. Therefore, it is still a challenge for the fabrication of monodispersed uniform CDs with excellent optical performance through facile solid phase reactions with low cost.

In the present work, we select the classical mesoporous molecular sieve SBA-15 as the template for solid state synthesis of CDs,

---

* Corresponding author.
E-mail address: hmxiong@fudan.edu.cn (H. Xiong).

https://doi.org/10.1016/j.cclet.2022.05.074

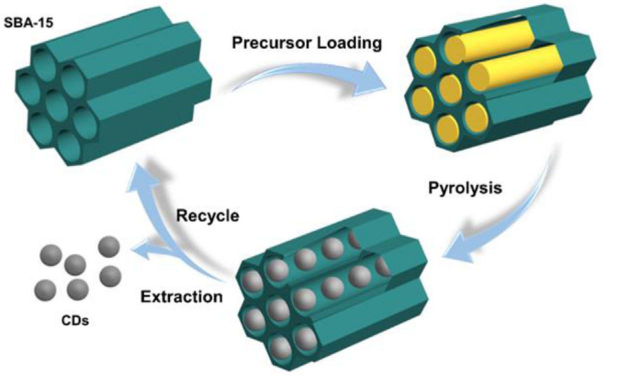

Scheme 1. Solid phase synthesis route of CDs employing SBA-15 as the template.

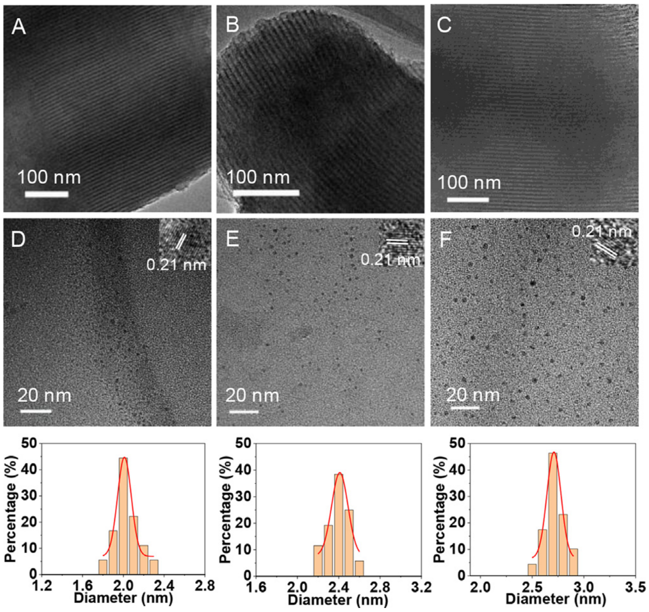

Fig. 1. TEM images of (A) SBA-15-A, (B) SBA-15-B and (C) SBA-15-C, respectively. TEM images and the corresponding particle size distributions of (D) Sample A, (E) Sample B and (F) Sample C, respectively.

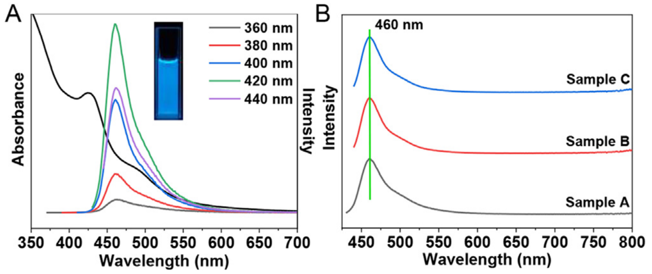

Fig. 2. (A) UV–vis absorption (black line) and fluorescence emission spectra (color lines, excited by different wavelengths of light) of CDs. Inset is the photograph of CDs solution under room light. (B) PL emission spectra of CDs under the excitation wavelength of 420 nm.

filling phenols and anilines into SBA-15 as single carbon sources, respectively. After pyrolysis in air at 200 °C for several hours, CDs formed in the channels of SBA-15, which can be easily extracted by ethanol with sonication. The remaining SBA-15 is recycled by annealing treatment in air for the next synthesis, while ethanol is recycled by evaporation and condensation. In this sustainable route, the preparation cost is greatly reduced and there are almost no waste to discharge. The as-prepared CDs have uniform sizes with very narrow distribution, high production yield over 65%, and quantum yield up to 88%. By adjusting the pore diameters of SBA-15, the particle sizes of the resulting CDs can be controlled precisely. Detailed characterizations confirm that, the emission wavelengths of such CDs are not determined by their sizes, but influenced by their composition and surface states, including oxygen/nitrogen contents, oxidation degree and graphitization degree.

A typical cycle route is illustrated in Scheme 1. Firstly, the saturated solution of a carbon source is soaked by SBA-15 and dried completely at room temperature. Then, the precursor is heated at 200 °C in air for several hours until CDs form in SBA-15 channels. After cooling down to room temperature, CDs are extracted from the template by ethanol with sonication, while the remaining SBA-15 with some residual carbon is calcined at 550 °C for the next synthesis. In comparison with other CDs preparation employing templates [29,31,34], our method shows significant advantages: (1) CDs can be extracted from the template and maintain their luminescent properties; (2) The template can be recycled for the successive syntheses, which does not influence the quality of the successive products; (3) The reaction conditions are mild and controllable; (4) Both the production yield and quantum yield of the CDs are high; (5) Many carbon sources can be applied in this route, and thus the as-prepared CDs exhibit adjustable properties.

To control the particle sizes of CDs, three kinds of SBA-15 were synthesized at different temperatures, resulting different pore diameters of 5.6 nm (SBA-15-A), 6.1 nm (SBA-15-B) and 6.7 nm (SBA-15-C), respectively. These diameters are calculated from the nitrogen adsorption/desorption isotherm curves in Fig. S1 (Supporting information), and the corresponding pore volumes are 0.79, 0.89 and 1.1 cm^3/g, respectively. The TEM images of these templates are shown in Fig. 1. Similar with the above calculation results, the pore diameters of SBA-15 templates observed by TEM are 5.8, 6.3 and 7.0 nm, respectively. Such uniform channels of SBA-15 ensure the uniformity of nanoparticle growth. But for a controlled nanoparticle synthesis, the homogeneity of nucleation is also important. There are several famous carbon source couples in literature, such as citric acid & ethylenediamine [16], citric acid & urea [35], and *o*-phenylenediamine & dopamine [36]. However, these couples are not suitable for our method, which needs to fill the pores homogeneously by ethanol solutions. When the ethanol solution dry and form precursors, different carbon sources will separate because of their different solubility, resulting in heterogeneous solid phases. Therefore, we use only one carbon source for each synthesis, which ensures the homogeneity of nucleation.

It is well known that phenols can dehydrate and anilines can deaminate at high temperate, respectively. Both of them will condensate into polymers, and carbonize to be the carbonized polymer dots with luminescent properties [37,38]. This process can be accelerated by SBA-15, a famous catalyst possessing highly ordered mesoporous structures (Fig. S2 in Supporting information). In a typical experiment, phloroglucinol is chosen as the carbon source which derives three kinds of CDs with diameters of 2.0 ± 0.2 nm (Sample A by SBA-15-A), 2.4 ± 0.2 nm (Sample B by SBA-15-B) and 2.7 ± 0.2 nm (Sample C by SBA-15-C), respectively. These samples are monodispersed spherical nanoparticles with lattice fringes of 0.21 nm, corresponding to the (100) plane of graphite. They have uniform sizes with very narrow distributions as proved by the TEM (Fig. 1) and AFM (Fig. S3 in Supporting information) results, indicating that the solid phase synthesis by mesoporous molecular sieves is able to control the nanoparticle sizes precisely.

The UV–vis absorption and photoluminescence (PL) emission spectra of the phloroglucinol derived CDs are shown in Fig. 2A. There is an obvious absorption peak at about 420 nm, corresponding to its strong blue emission at 460 nm. This PL emission peak keeps still when the excitation wavelength varies from 360 nm to 440 nm. It is interesting that all three samples show the same PL emission spectra in Fig. 2B, although their particle size increases from 2.0 nm to 2.7 nm. Their ethanol solution photos under room light and UV light are shown in Fig. S4 (Supporting information). Amazingly, these samples show bright blue fluorescence even under the room light. Under excitation light of 420 nm, their quantum yield are measured to be 87.6%, 88.4% and 87.8% by an integrating sphere, respectively, which is remarkable at present. It should be mentioned that the Raman spectra of these samples cannot be measured, because their fluorescence is too strong.

To explore the factors affecting the luminescence properties of CDs, these CDs were analyzed by infrared (IR) measurement and X-ray photoelectron spectroscopy (XPS). Fig. S5 (Supporting information) shows the three samples have almost the same IR spectra, exhibiting O−H bond vibration at 3420 cm^{-1}, C=C bond vibration at 1615 cm^{-1}, and C−O bond vibration at 1151 cm^{-1}, *etc.* The IR results confirm that only dehydration took place among phloroglucinol molecules, and no solvents were involved in this solid phase synthesis. In addition, a tiny IR band is observed at 1789 cm^{-1}, representing C=O bond vibration which may be caused by air oxidation. Fig. S6 (Supporting information) illustrate the XPS survey spectra of these samples, which have the same atom ratios of C 1s (285 eV) and O 1s (533 eV). In Fig. S7 (Supporting information), the deconvoluted curves of C 1s have three components of C=C (284.6 eV), C−O (286.2 eV) and C=O (288.5 eV), while those of O 1s are composed of C−O (533.0 eV) and C=O (531.6 eV). Table S1 (Supporting information) compares all the above components of the three samples, which confirms that these CDs have the same composition.

The relationships between CDs fluorescence and their structures are controversial for years. There are several popular models to demonstrate such relationships. The first is the classical quantum size effect [39], which requires the CDs to be single nanocrystals with no defects and almost no surface groups. Some carbon quantum dots fit this rule in literature [40], but obviously our CDs cannot be sorted into this group. The second model is called molecular fluorescence which arise from the organic fluorescent groups on CDs [41]. As for our samples, IR spectra prove the organic groups on CDs surfaces are much simpler than those organic dyes, and the UV–vis curve show the continuous absorption from UV to visible region that is not the feature of organic fluorescent molecules. Hence, our samples cannot be ascribed to this model either. The third one is that, in many carbonized polymer dots the polymer chains and the carbonized cores crosslink with each other, so fluorescence is determined by the sp^2 and sp^3 domains together [42]. However, since we cannot measure the Raman spectra of these samples, such information is not available. The fourth mechanism is the surface states controlled fluorescence [43]. In this model, CDs are composed of graphite fragments containing defects, heteroatoms and organic groups. Because CDs are so small that XPS measurement is able to gather all information in both the cores and the surfaces, the fluorescence of CDs which is determined by the states of all atoms synergistically can be interpreted by the XPS results. In order to verify this hypothesis, we should change the composition of CDs solely and see what will happen to their fluorescence.

Resorcinol, *o*-phenylenediamine and *p*-phenylenediamine were selected as single carbon sources to synthesize CDs, respectively. After the same preparation process, green, yellow and red emissive CDs were obtained and designated as G-CDs, Y-CDs and R-CDs, respectively. In Fig. 3, the TEM images show these samples have the same particle sizes of about 2.7 nm, and the same lattice spacing of 0.21 nm corresponding to the (100) plane of graphite. The height measurement by AFM also verifies the uniform sizes of these samples (Fig. S8 in Supporting information). Their XRD patterns in Fig. S9 (Supporting information) are similar, with a wide diffraction peak at 24° corresponding to the (002) crystal plane of graphite. Fig. 4 shows their fluorescence emission spectra under different wavelengths of excitation light. As the excitation wavelength varies, both G-CDs and R-CDs show excitation-independent PL emission wavelengths, while the emission wavelength of Y-CDs moves slightly. These samples emit bright fluorescence under UV light, with quantum yield of 28.8%, 21.3% and 14.6%, respectively. The above results prove that the fluorescence properties of our CDs are mainly determined by the carbon sources, but not the particle sizes. Through changing the carbon source, the PL emission of CDs can be tuned from blue (460 nm) to red (605 nm). With this respect, doping CDs with nitrogen has made a significant contribution. It can be expected that near IR emissive CDs will be obtained in this way when a suitable carbon source is found.

IR and XPS measurement were also carried out for these CDs. Fig. S10 (Supporting information) reveals that G-CDs have O−H (stretching at 3416 cm^{-1}), C=C (stretching at 1616 cm^{-1}), C−H (bending at 1381 cm^{-1}) and C−O (stretching at 1092 cm^{-1}) groups. Both Y-CDs and R-CDs show similar O−H band at 3405 cm^{-1}, N−H band at 3206 cm^{-1}, C−H band at 2925 cm^{-1}, C=N band at 1617 cm^{-1} and C=C band at 1508 cm^{-1}, respectively. The existence of N−H and C=N bonds demonstrate that, the carbon source anilines are able to dope nitrogen into the CDs structure in the present solid phase synthesis. Fig. S11 (Supporting information) compares the XPS data of the three samples. G-CDs have 68.33% of carbon and 31.67% of oxygen, Y-CDs have 77.76% of carbon, 14.24% of oxygen and 7.99% of nitrogen, and R-CDs have 67.16% of carbon, 26.36% of oxygen and 6.48% of nitrogen, respectively. In the high resolution spectra, the O 1s bands of these samples are also deconvoluted to be C−O bond at 533.0 eV and C=O bond at 531.6 eV. Particularly, the high resolution N 1s bands of Y-CDs and R-CDs are deconvoluted to be graphite nitrogen at 401.8 eV, amino nitrogen at 399.8 eV and pyridine nitrogen at 398.2 eV, respectively.

Since the sizes of CDs are only several nanometers, XPS is able to detect the whole composition of both the surfaces and the cores, including the elements and their valence states. Therefore, the relationship between CDs composition and fluorescence can be interpreted by the XPS results. In Tables S2 and S3 (Supporting information), Sample C is designated as B-CDs for comparison with G-CDs, Y-CDs and R-CDs, because all of them are synthesized from SBA-15-C and have the same size of about 2.7 nm. According to previous reports, the increase of oxidation state and graphite nitrogen content will cause fluorescence redshift of CDs [43–46]. Therefore, the fluorescence redshift from B-CDs to G-CDs can be ascribed to the oxygen species improvement, the fluorescence redshift from G-CDs to Y-CDs is due to nitrogen doping, and the fluorescence redshift from Y-CDs to R-CDs is based on the increase of the graphite nitrogen, respectively. Such a mechanism is illustrated in Scheme 2, which points out a direction to regulate CDs fluorescence by changing their composition.

An outstanding merit of this work is that the template SBA-15 can be recycled. In most of the previous research, the templates should be decomposed by acids or alkalis to collect CDs, which not only raises the cost of fabrication, but also increases difficulties in product purification [28,47,48]. In our present work, the ethanol extraction can collect most of the CDs in SBA-15 channels, while the remaining SBA-15 can be easily recycled by calcination in a furnace for 5 h under the air atmosphere at 550 °C. After calcination, the color of SBA-15 returns to white, and the retention rate of weight is over 90%. The TEM image (Fig. S12A in Supporting information) shows the recycled SBA-15 still maintains its ordered mesoporous structure, while the low-angle XRD patterns (Fig. S12B in Supporting information) of the original SBA-15 and the recycled SBA-15 are almost the same, exhibiting the strong (100) diffraction peak and the weak (110) and (200) diffraction peaks, respec-

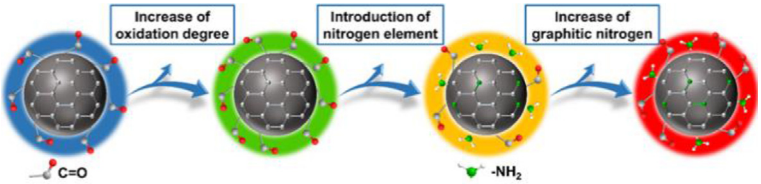

Scheme 2. Possible relationships between the PL colors and the composition of CDs.

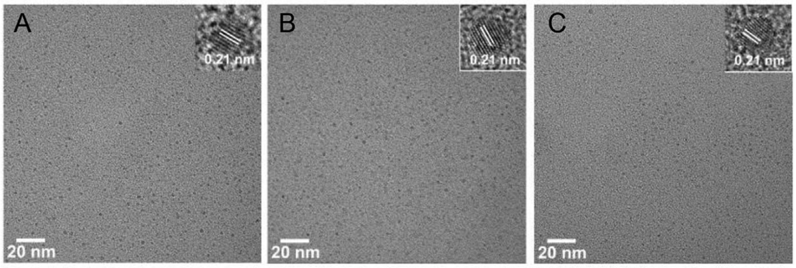

Fig. 3. TEM images of (A) G-CDs, (B) Y-CDs and (C) R-CDs, with their inset HRTEM images, respectively.

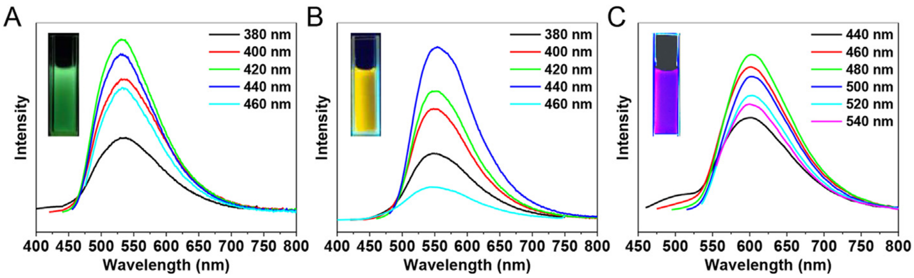

Fig. 4. PL emission spectra of the ethanol solutions of CDs under different wavelengths of excitation light from resorcinol (A), *o*-phenylenediamine (B) and *p*-phenylenediamine (C), with the inset photos under UV light.

tively. These results confirm that after reaction as the template and calcination at high temperature, SBA-15 has recovered completely for the next synthesis. Even after 10 times of recycling, the nitrogen adsorption/desorption isotherm curves of the recycled SBA-15 kept unchanged in comparison with the original SBA-15 (Fig. S13A in Supporting information). Using such a recycled SBA-15 as the template and phloroglucinol as the carbon source, the as-prepared CDs show the same PL emission spectra (Fig. S13B in Supporting information) as those of the initially synthesized CDs. Since the price of SBA-15 is much higher than those of carbon sources and ethanol, our route greatly cuts down the cost of CDs preparation.

In summary, we invent a recyclable solid phase method to synthesize full color emissive CDs, employing SBA-15 as the template and phenols or anilines as the single carbon sources. This method has many advantages, such as high yield, low cost, convenient operation, safe production and green chemistry. The as-prepared CDs have uniform sizes, strong fluorescence, good dispersibility and high purity. The CDs particle sizes are controlled by adjusting the pore diameters of SBA-15, and the results show the PL emission of CDs does not shift with the change of particle sizes. But the fluorescence of CDs can be easily controlled by changing the carbon sources. FTIR and XPS analyzes prove that the fluorescence properties are based on the composition of CDs, but not the particle sizes, which is quite different from the quantum size effects. Since this method has greatly accelerated the CDs preparation process, we believe CDs with special structures and rich properties will be discovered in this way soon.

Declaration of competing interest

The authors declare that they have no known competing financial interests or personal relationships that could have appeared to influence the work reported in this paper.

Acknowledgments

This work was financially supported by the National Natural Science Foundation of China (Nos. 21975048, 21771039), and the Shanghai Science and Technology Committee (No. 19DZ2270100).

Supplementary materials

Supplementary material associated with this article can be found, in the online version, at doi:10.1016/j.cclet.2022.05.074.

References

[1] X. Yang, L. Sui, B. Wang, et al., Sci. China Chem. 64 (2021) 1547–1553.
[2] X. Dong, X. Niu, J. Wei, H. Xiong, Chem. J. Chin. Univ. 40 (2019) 1288–1292.
[3] F. Yuan, P. He, Z. Xi, et al., Nano Res. 12 (2019) 1669–1674.
[4] B. Wang, J. Li, Z. Tang, B. Yang, S. Lu, Sci. Bull. 64 (2019) 1285–1292.
[5] S. Sun, L. Zhang, K. Jiang, A. Wu, H. Lin, Chem. Mater. 28 (2016) 8659–8668.
[6] Z. Tang, Z. Lin, G. Li, Y. Hu, Anal. Chem. 89 (2017) 4238–4245.
[7] H. Zhang, Y. Chen, M. Liang, et al., Anal. Chem. 86 (2014) 9846–9852.
[8] X. Sun, J. He, Y. Meng, et al., J. Mater. Chem. A 4 (2016) 4161–4171.
[9] X. Xu, R. Ray, Y. Gu, et al., J. Am. Chem. Soc. 126 (2004) 12736–12737.
[10] B. Wang, S. Lu, Matter 5 (2022) 110–149.
[11] H. Liu, T. Ye, C. Mao, Angew. Chem. Int. Ed. 46 (2007) 6473–6475.
[12] L. Bao, Z.L. Zhang, Z.Q. Tian, et al., Adv. Mater. 23 (2011) 5801–5806.

[13] X. Tan, Y. Li, X. Li, et al., Chem. Commun. 51 (2015) 2544–2546.
[14] J. Wang, C.F. Wang, S. Chen, Angew. Chem. Int. Ed. 124 (2012) 9431–9435.
[15] B. Wang, J. Yu, L. Sui, et al., Adv. Sci. 8 (2021) 2001453.
[16] S. Zhu, Q. Meng, L. Wang, et al., Angew. Chem. Int. Ed. 52 (2013) 3953–3957.
[17] X. Xu, L. Mo, W. Li, et al., Chin. Chem. Lett. 32 (2021) 3927–3930.
[18] S. Qu, X. Wang, Q. Lu, X. Liu, L. Wang, Angew. Chem. Int. Ed. 51 (2012) 12215–12218.
[19] L. Pan, S. Sun, A. Zhang, et al., Adv. Mater. 27 (2015) 7782–7787.
[20] X. Niu, T. Song, H. Xiong, Chin. Chem. Lett. 32 (2021) 1953–1956.
[21] Z. Zhu, R. Cheng, L. Ling, Q. Li, S. Chen, Angew. Chem. Int. Ed. 59 (2020) 3099–3105.
[22] Z. Kang, S.T. Lee, Nanoscale 11 (2019) 19214–19224.
[23] B. Wang, H. Song, Z. Tang, B. Yang, S. Lu, Nano Res. 15 (2022) 942–949.
[24] H. Ding, J.S. Wei, P. Zhang, et al., Small 14 (2018) 1800612.
[25] A.B. Bourlinos, A. Stassinopoulos, D. Anglos, et al., Small 4 (2008) 455–458.
[26] A.B. Bourlinos, A. Stassinopoulos, D. Anglos, et al., Chem. Mater. 20 (2008) 4539–4541.
[27] R. Liu, D. Wu, S. Liu, et al., Angew. Chem. Int. Ed. 48 (2009) 4598–4601.
[28] Z.G. Gu, D.J. Li, C. Zheng, et al., Angew. Chem. Int. Ed. 56 (2017) 6853–6858.
[29] M.C. Ortega-Liebana, N.X. Chung, R. Limpens, et al., Carbon 117 (2017) 437–446 N Y.
[30] Y. Yang, D. Wu, S. Han, P. Hu, R. Liu, Chem. Commun. 49 (2013) 4920–4922.
[31] A.J. Amali, H. Hoshino, C. Wu, M. Ando, Q. Xu, Chem. Eur. J. 20 (2014) 8279–8282.
[32] Y. Mu, N. Wang, Z. Sun, et al., Chem. Sci. 7 (2016) 3564–3568.
[33] C. Wang, Y. Chen, Y. Xu, et al., ACS Appl. Mater. Interfaces 12 (2020) 10791–10800.
[34] J. Liu, N. Wang, Y. Yu, et al., Sci. Adv. 3 (2017) e1603171.
[35] Y. Zhao, B. He, E. Liu, et al., J. Phys. Chem. Lett. 12 (2021) 4530–4536.
[36] S. Lu, L. Sui, J. Liu, et al., Adv. Mater. 29 (2017) 1603443.
[37] S. Ghosh, H. Ali, N.R. Jana, ACS Sustain. Chem. Eng. 7 (2019) 12629–12637.
[38] H. Ding, X.X. Zhou, Z.H. Zhang, et al., Nano Res. 15 (2022) 3548–3555.
[39] H. Li, X. He, Z. Kang, et al., Angew. Chem. Int. Ed. 49 (2010) 4430–4434.
[40] F. Yuan, T. Yuan, L. Sui, et al., Nat. Commun. 9 (2018) 2249.
[41] Y. Song, S. Zhu, S. Zhang, et al., J. Mater. Chem. C 3 (2015) 5976–5984.
[42] S. Tao, T. Feng, C. Zheng, S. Zhu, B. Yang, J. Phys. Chem. Lett. 10 (2019) 5182–5188.
[43] H. Ding, S.B. Yu, J.S. Wei, H.M. Xiong, ACS Nano 10 (2016) 484–491.
[44] C. Liu, L. Bao, M. Yang, et al., J. Phys. Chem. Lett. 10 (2019) 3621–3629.
[45] S. Sarkar, M. Sudolská, M. Dubecký, et al., J. Phys. Chem. C 120 (2016) 1303–1308.
[46] K. Holá, M. Sudolská, S. Kalytchuk, et al., ACS Nano 11 (2017) 12402–12410.
[47] H. Zhang, K. Liu, J. Liu, et al., CCS Chem. 2 (2020) 118–127.
[48] H. Chen, G.D. Wang, X. Sun, et al., Adv. Funct. Mater. 26 (2016) 3973–3982.